

Article

Methodology for Circuit Breaker Contact Diagnosis through Dynamic Resistance Measurements and Fuzzy-Logic-Based Analysis

Ronimack T. Souza ^{1,*}, George R. S. Lira ¹, Edson G. Costa ¹, Adriano C. Oliveira ²
and Antonio F. Leite Neto ³

¹ Department of Electrical Engineering, Federal University of Campina Grande, Aprigio Veloso St., 882, Campina Grande 58429-900, Brazil; george@dee.ufcg.edu.br (G.R.S.L.); edson@dee.ufcg.edu.br (E.G.C.)

² Engineering Department, Federal Rural University of the Semi-Arid, Francisco Mota St., Caraubas 59780-000, Brazil; adriano.costa@ufersa.edu.br

³ Postgraduate Program in Electrical Engineering, Federal University of Campina Grande, Campina Grande 58428-830, Brazil; antonio.leite@ee.ufcg.edu.br

* Correspondence: ronimack@dee.ufcg.edu.br; Tel.: +55-83-2101-1140

Abstract: This paper presents a methodology capable of measuring, processing, and extracting contact resistance parameters that enable the identification of the contact degradation level inside arc extinction chambers in medium- and high-voltage circuit breakers (CB). To determine the contact degradation level, an algorithm was developed to extract the characteristic parameters from the results of dynamic resistance measurement (DRM). To analyze the dataset parameters, this work employs the combination of different statistical tools, such as boxplots and fuzzy logic, enabling the evaluation to be conducted without the subjectivity inherent in human decision. Therefore, a more objective and reliable diagnosis could be achieved. The DRM tests were performed on two types of minimum-oil CB (MOCB), 800 A/15 kV/12.5 kA (CB-A) and 2000 A/72.5 kV/31.5 kA (CB-B and CB-C). For CB-A and CB-B, three contacts were utilized for each CB, with significant contact degradation. For CB-C, a single contact was employed without significant degradation. The DRM curves of the CB-C contact were used as the reference for evaluation of the CB-B contacts. For this purpose, a new DRM system was developed. The proposed methodology can be defined as a complement for other diagnostic techniques, serving as a non-subjective asset management tool, supporting decisions regarding equipment interventions.

Keywords: monitoring; diagnostic; circuit breakers; fuzzy logic; statistical analysis; dynamic resistance



Citation: Souza, R.T.; Lira, G.R.S.; Costa, E.G.; Oliveira, A.C.; Leite Neto, A.F. Methodology for Circuit Breaker Contact Diagnosis through Dynamic Resistance Measurements and Fuzzy-Logic-Based Analysis. *Energies* **2024**, *17*, 1869. <https://doi.org/10.3390/en17081869>

Academic Editors: Zhijin Zhang and Hualong Zheng

Received: 4 March 2024

Revised: 2 April 2024

Accepted: 7 April 2024

Published: 14 April 2024



Copyright: © 2024 by the authors. Licensee MDPI, Basel, Switzerland. This article is an open access article distributed under the terms and conditions of the Creative Commons Attribution (CC BY) license (<https://creativecommons.org/licenses/by/4.0/>).

1. Introduction

Circuit breakers (CBs) are protective electromechanical equipment designed to conduct, re-establish, and interrupt electrical currents at a certain point of a circuit. Generally, they are used to isolate a circuit section in case of overloads or fault currents due to short circuits. CB malfunctioning might provoke serious problems in electrical systems, such as a large area without power delivery or a CB explosion (with its respective consequences).

During the CB breaking operations, the arcing contact (AC) is slightly ablated due to the electric arc effects. The ablation makes the contact increasingly short [1]. Therefore, the ablation/degradation of the AC is a critical parameter for CB condition monitoring [2].

Condition-based monitoring (CBM) can more accurately estimate the degree of CB wear-out [3]. Other studies [3–6] have proposed analyzing CBs using various characteristic parameters and the application of CBM techniques. Specifically, for analyzing the contact operating status, most electric companies use static resistance measurement (SRM) to assess the CB contact degradation level. However, this technique can only analyze the main contacts (MC), failing to provide information regarding the arcing contacts (AC). Furthermore, this procedure is often carried out using inadequate test equipment [7–12].

For these reasons, the need arises for the application of more efficient monitoring techniques capable of accurately evaluating the chamber operating state. In the last two decades, research has been directed towards contact DRM as a way of evaluating both the AC and the MC. During DRM tests, a resistance curve is generated. From the DRM curves, the main and arcing contact resistances can be assessed individually, allowing the evaluations of all parts of the contacts [7–9].

In recent years, several studies have been developed on this theme [4–22]. However, these studies do not present an agreed methodology for measurement and analysis to define reference parameters to correlate the DRM results to the level of contact wear. Parameters such as timing measurements, travel curve measurement, and dynamic resistance measurement are utilized by references [4,7,14–18,22], timing measurements, travel curve measurement, and contact temperature are used by reference [5], dynamic resistance measurement is used by references [7–13,20,21], and dynamic resistance measurement and vibration analysis are used by references [7,10,11].

Moreover, it was reported by [8,19,21,22] that DRM curves obtained at the rated speed of contacts opening are not reproducible from one test to another. In addition, the research conducted by [23–25] included experimental studies, and the authors developed measurement systems to diagnose the contact ablation status.

In the work of [26], an analysis was conducted on alternative parameters extracted from the DRM technique, such as amplitude and variance. These parameters provided reliable diagnostics for the contact degradation level, verified through visual inspection of the contacts. In [27], the results of various faults inserted into a CB were investigated through multi-physical simulations and experiments, identifying that DRM exhibits specific behavior for each type of failure.

DRM parameters are used to estimate the contact degradation level. However, this process is not trivial, since technical managers must make use of assumptions, approximations, or simplifications. Thus, this study presents a new methodology for measuring, processing, and extracting DRM parameters and a system to support decision-making. For the developed methodology, the boxplot statistical method is proposed to deal with the effects of the DRM curve variations during the global analysis of DRM parameters.

The particularity of this work compared to others lies in the utilization of two complementary techniques to analyze the DRM parameters in order to estimate the degradation level of CB contacts. In the first analysis, a boxplot was employed to define the value that best represents a set of data points, and then fuzzy logic was employed to estimate the level of contact degradation.

In addressing the subjective judgment, uncertainty, and imprecision during the decision-making process, adaptive tools for uncertainty situations are necessary. Accordingly, fuzzy logic was employed to provide more reliable, and accurate results. The choice to use fuzzy logic was made due to the limited quantity of available CB samples for research purposes. According to [5], diagnosis using fuzzy logic overcomes the difficulties that expert systems present in acquiring knowledge; for example, neural networks require a large number of data to be trained. The main advantage of system diagnosis based on fuzzy models is that it allows the adoption of a limited number of input data while focusing on the essential characteristics of the device being tested, thereby considering the uncertainties and inaccuracies associated with all input data.

This system enables the classification of contact degradation level in medium- and high-voltage CBs. This method is applicable to CBs in operation and can maximize operational time and minimize maintenance costs, thereby assisting in maintenance scheduling and supporting maintenance crews in decision-making regarding the need for interventions.

2. Proposed Technique

The proposed technique presented in this study comprises the integration of a measurement technique with a post-processing procedure applied to the measured signals, providing a comprehensive and reliable diagnostic of CB extinction chambers. The tech-

nique is based on the DRM and serves as the basis for the boxplot analysis, which functions as a parameter extraction tool. Subsequently, these parameters are used as input variables of a fuzzy logic algorithm designed to provide the final diagnosis. The schematic diagram presented in Figure 1 represents the proposed methodology.

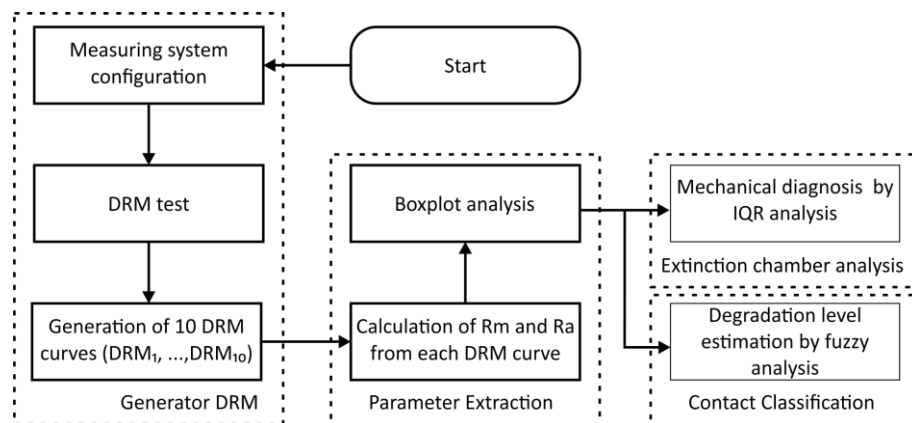


Figure 1. Block diagram of the proposed diagnostic technique.

2.1. Data Acquisition

The data acquisition technique selected for the proposed methodology is DRM. Two CB models were used in this research, a medium-voltage and two high-voltage MOCBs. The specifications of the used CBs are as follows:

- CB-A-MOCB of 800 A/15 kV/12.5 kA;
- CB-B-MOCB of 2000 A/72.5 kV/31.5 kA;
- CB-C-MOCB of 2000 A/72.5 kV/31.5 kA.

The CB contacts were previously degraded due to electrical, mechanical, and thermal stress in service. In order to provide grants for the diagnosis of CBs, DRM tests were performed on samples CB-A, CB-B, and CB-C. The tests aimed to identify, from the results obtained, which DRM characteristic parameters can be monitored for quantifying the contact degradation level.

To conduct contact resistance tests on circuit breakers, a system developed for this purpose was adopted, as depicted in Figure 2. The system consists of a stationary battery of 12 V/220 Ah serving as a current source and resistors produced from Kanthal DS wires (Cr-Al-Fe) to limit the test current from the battery. To measure the voltage and current signals in the CB, a 2-channel digital oscilloscope was used. The current signal is obtained from a current shunt (500 A/60 mV) and a DC-DC analog voltage transducer (0–60 mV/0–5 V), model W153, manufactured by Kron Instrumentos Elétricos Ltda., São Paulo, SP, Brazil. The output signal from the voltage transducer is sent to channel 1 of the oscilloscope through a 200 MHz/300 V voltage probe, model P2220, manufactured by Tektronix Inc., Beaverton, OR, USA. The voltage signal obtained at the circuit breaker terminals is sent to channel 2 of the oscilloscope through a second 200 MHz/300 V voltage probe, model P2220. A schematic diagram of the selected DRM system is shown in Figure 2. The measuring system has the following capabilities:

- Direct current injection of up to 300 A (voltage source: 12 V stationary battery);
- Adjustment of the battery current through Cr-Al-Fe resistor (40 mΩ–1.3 Ω/4 kW);
- Measurement of the current with current shunt (500 A/60 mV) and voltage/voltage transducer (60 mV/5 V) and voltage probe;
- Acquisition of the information captured in the DRM (current and voltage drop across the contacts) using voltage probes and digital oscilloscope.

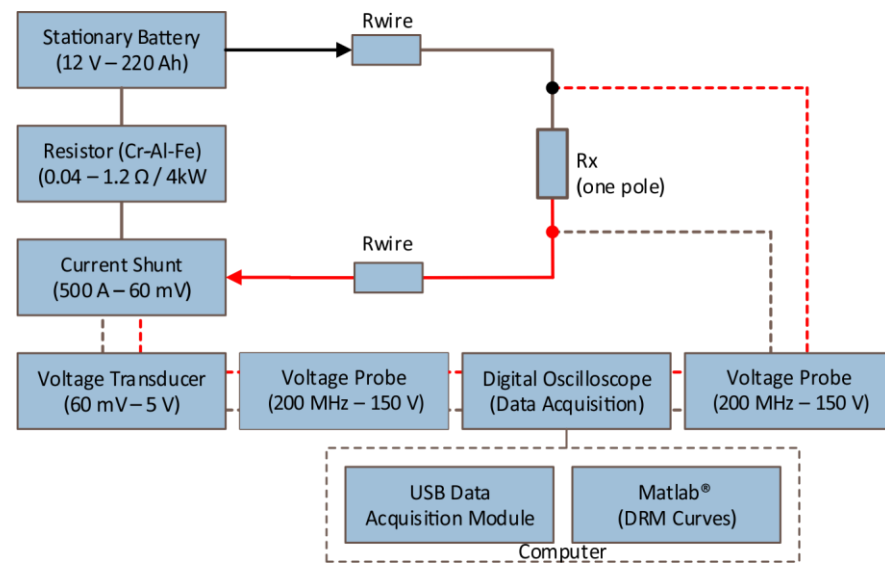


Figure 2. Block diagram of the DRM system—adapted from [17].

In Figure 3, a typical DRM curve is presented in which the resistance regions regarding the main and arcing contacts are indicated. The parameter R_m is the resistance of the main contact, determined with the contacts completely closed. The parameter R_a is the average resistance of the arcing contact, determined as the average of the resistances related to the arcing contact region. The transition zone between these regions (R_t) were not considered in the calculation of the parameter R_a since it is possible that mechanical imperfections in the contact surface produce small separations of the contacts during the opening process, generating masked resistance values.

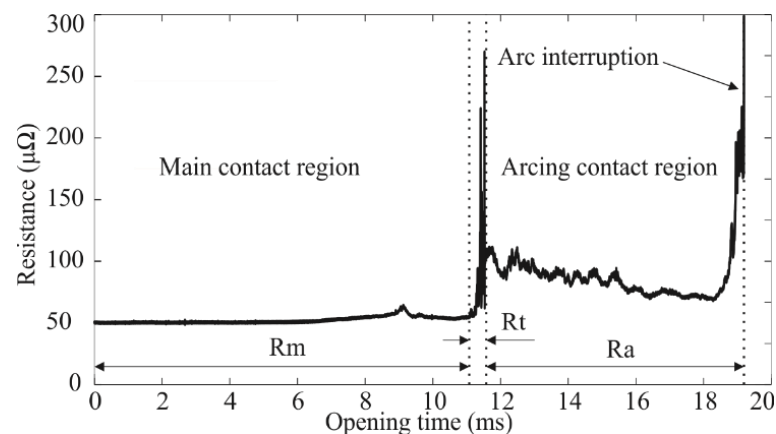


Figure 3. Typical DRM curve.

The parameters R_m and R_a were obtained through the following procedure:

- Calculation of the mean resistance on the main contact region (R_m) considering the first 1000 samples;
- Identification of the main contact separation instant by locating a resistance increase of 5% from the calculated R_m value;
- Identification of the arcing contact separation instant by locating a resistance increase of 500% from the calculated R_m value;
- Classification of the initial 10% of the arcing contact region as a transition zone, in which mechanical imperfections may cause measurement errors;
- Calculation of the mean resistance on the arcing contact region (R_a), disregarding the transition zone.

To evaluate the contacts, each CB pole was subjected to 10 DRM tests. For each DRM curve, the parameters R_m and R_a were extracted. Afterwards, the obtained dataset underwent an analysis that used boxplots to define the best values to represent the R_m and R_a from each contact.

The DRM tests were conducted in the laboratory on CB-A and CB-B, for which photographs of the laboratory setup are shown in Figures 4 and 5, respectively. Subsequently, the poles of each CB were dismantled in order to evaluate the relationship between the DRM curves and the contact degradation level (visually assessed).

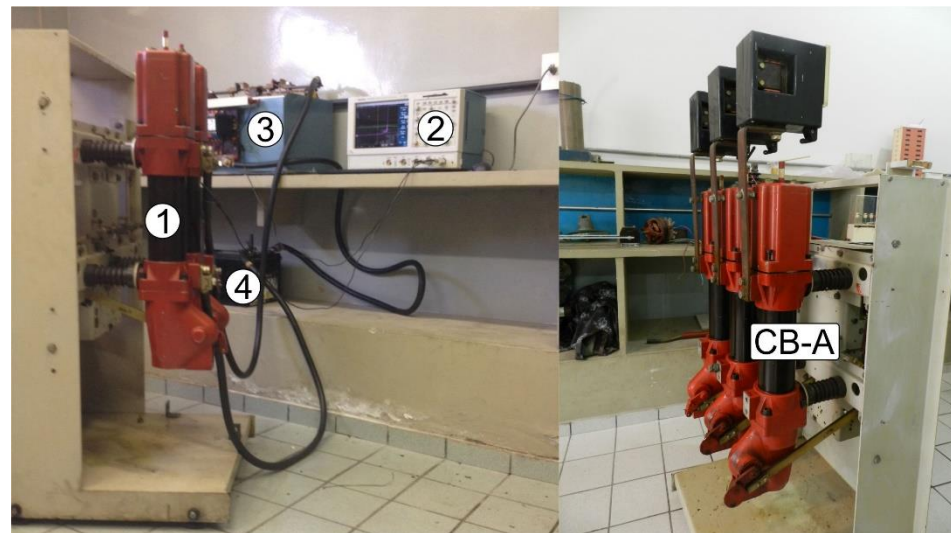


Figure 4. Laboratory setup of DRM in circuit breaker CB-A. 1—MOCB; 2—oscilloscope; 3—resistor, current shunt, voltage transducer; and 4—stationary battery.



Figure 5. Laboratory setup of DRM in circuit breakers CB-B and CB-C. 1—MOCB; 2—oscilloscope; 3—resistor, current shunt, voltage transducer; and 4—stationary battery.

The contacts of CB-A were labeled as CB-A1, CB-A2, and CB-A3. Photographs of these fixed and mobile contacts, from left to right, respectively, are shown in Figure 6. Similarly, the contacts of CB-B were labeled as CB-B1, CB-B2, and CB B3. In Figure 7, photographs of the fixed and mobile contacts from CB-B are depicted, with AC being the arcing contact and MC the main contact.



Figure 6. Samples of contacts CB-A1, CB-A2, and CB-A3, from left to right, respectively.

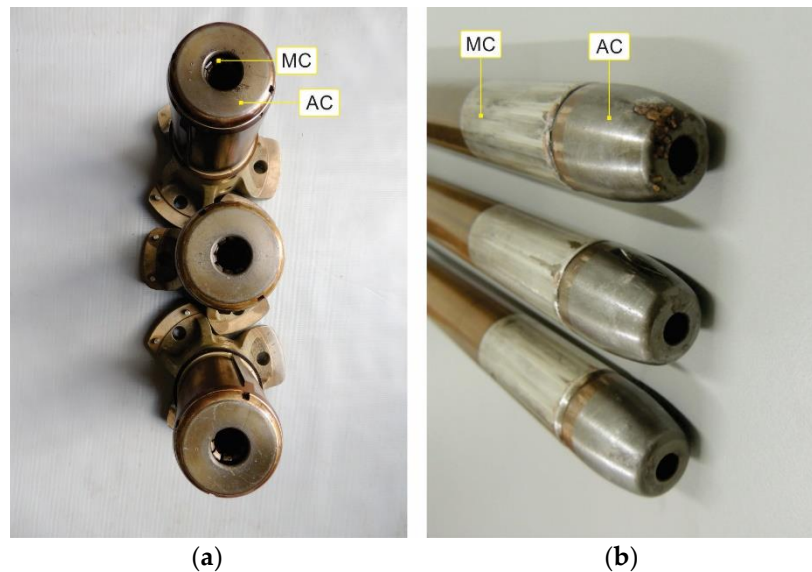


Figure 7. Samples of contacts CB-B1, CB-B2, and CB-B3, from bottom to top, respectively. (a) Fixed contact; (b) moved contact.

Subsequently, another contact (CB-C1) without significant degradation from a third CB, named CB-C, was submitted to DRM studies. Its DRM curves were the reference for evaluation of the CB-B contacts. To reduce the risks of fault insertion, the CB-C was not dismantled.

2.2. Parameter Extraction

In this section, the procedure employed for data analysis and DRM parameter extraction is presented. The boxplot analysis was the chosen method since this approach allows the visualization, comparison, and measurement of the data dispersion, symmetry, and behavior [28].

The boxplot is defined in terms of five quantities/statistics: minimum value of the dataset, maximum value of the dataset, Q2 (median value of the dataset), Q1 or first quartile (the dataset sample that has 25% of the data at or below it), and Q3 or third quartile (the dataset sample that has 75% of the data at or below it). In Figure 8, a typical representation of the boxplot chart is shown.

Additionally, the boxplot encompasses the following characteristic parameters: the interquartile range (IQR), upper limit (UL), lower limit (LL), and outliers. The IQR is estimated by the difference between the third and first quartiles ($Q3 - Q1$), which serves as a metric of sample dispersion. The UL ($Q3 + 1.5(Q3 - Q1)$) and LL ($Q1 - 1.5(Q3 - Q1)$) define values from which the samples are considered possible outliers. The outliers might indicate samples that were incorrectly measured or recorded, but they may also indicate exceptional behaviors in the dataset.

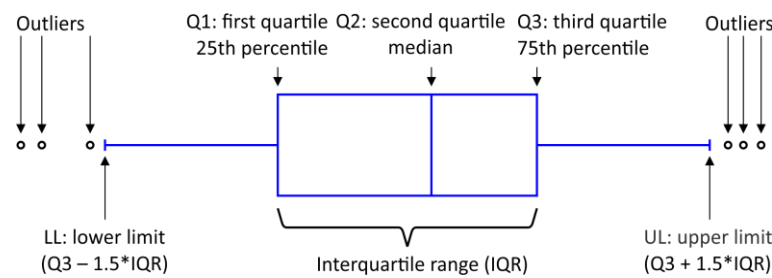


Figure 8. Typical representation of the boxplot chart.

Thus, the boxplot analysis was applied to the datasets composed of the R_m and R_a parameters from each CB. The third quartile was adopted as an input parameter of the decision-making tool because it represents most of the measured data, ensuring that decisions cover the general behavior of the data. Variations in the median and IQR values can also indicate failures in the CB poles, as will be shown later.

2.3. Contact Classification

The classification of the contact degradation level is often not trivial or even simple to evaluate since there are numerous factors that can influence the final decision on the contact status, such as contact vibration, test current level, and the state of the extinction medium. Regardless of the analyzed equipment, the consideration of factors with some degree of uncertainty depends on prior knowledge of these factors, for which approximations and calculations can be used to achieve a mathematical model, providing a relevant conclusion [29–33]. For the troubleshooting of these peculiarities, fuzzy logic has been applied to the data processing.

The developed fuzzy-logic-based system aims to quantify the contact degradation level considering the DRM characteristic parameters and CB characteristics. Two parameters were established in the configuration of the fuzzy system. The first concerns the manufacturer-recommended limits for contact resistances according to the CB characteristics. The second concerns the importance attributed to each of the processing rules considering operating time, operating conditions, and how critical the CB is to the electrical system. The correct system configuration will provide more reliable results, thereby providing more reliable diagnosis for the equipment operating status.

When assessing the implementation of the proposed methodology, the fuzzy system developed and presented in [34] was utilized, as depicted in Figures 9–11. The Q3 values of the parameters R_m and R_a , obtained from the boxplot analysis, are the fuzzy system input data. For each value of R_m and R_a , at least one input membership function is activated. As described in [34], five linguistic input variables were established for the proposed system, designated as Low (L); Moderately Low (ML); Median (M); Moderately High (MH); and High (H).

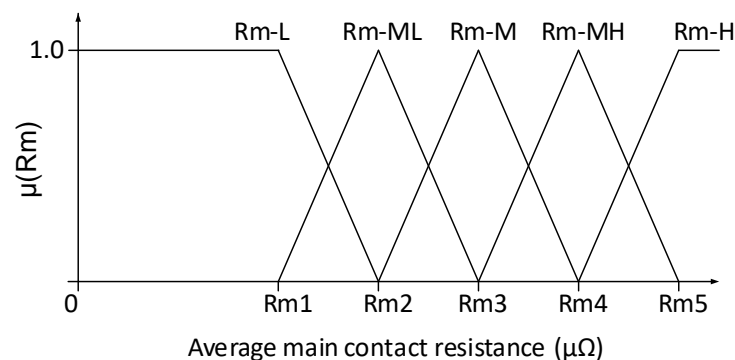


Figure 9. Membership functions of linguistic variables of R_m entry [34].

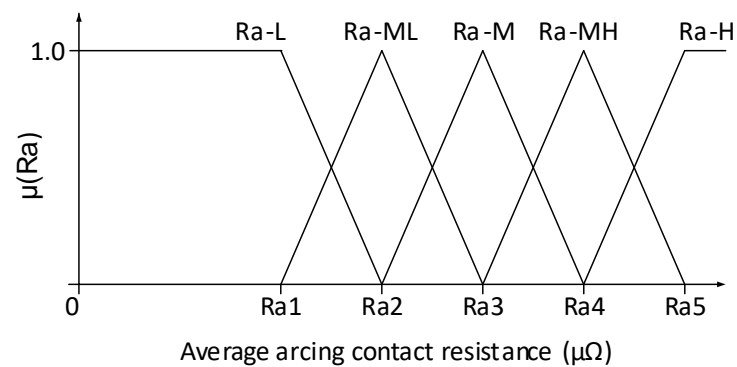


Figure 10. Membership functions of linguistic variables of Ra entry [34].

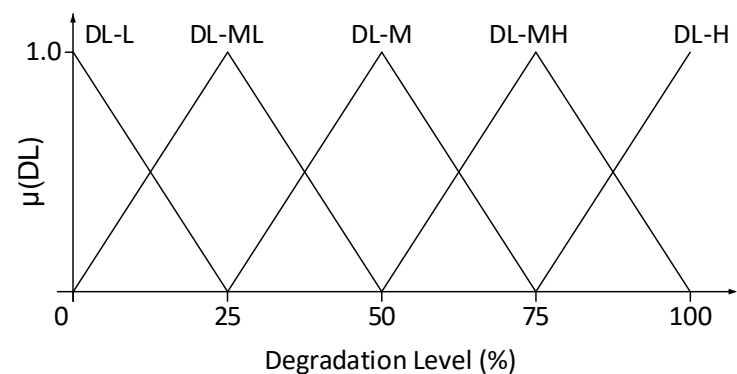


Figure 11. Membership functions of linguistic variables DL output [34].

The weights of the maximum interval and the formats of the input and output membership functions were heuristically defined considering that the contact degradation increases linearly and that it is directly proportional to the contact resistance value; thus, it can be represented by linear functions. For all linguistic variables, an overlap of 50% was established. A graphic illustration of membership functions representing each linguistic variable depending on R_m and R_a entries is presented in Figures 9 and 10, respectively.

To estimate the degradation level of each contact, the standard values adopted as reference were the maximum contact resistances provided by the default values of [35]. In the parametrization of the fuzzy system and for the definition of the fuzzy rules, first, the contact resistance limits in the main and arcing contacts regions were established. For sample A, the resistance of the main contact region ranges from 150 $\mu\Omega$ to 300 $\mu\Omega$ for a new and a degraded contact, respectively. For samples B and C, the resistance of the main contact region ranges from 40 $\mu\Omega$ to 80 $\mu\Omega$ for a new and a degraded contact, respectively.

As there is no reference in the literature for the resistance of the arcing contact region, values from laboratory tests were adopted. In these cases, it was estimated that, for sample A, the resistance of the arcing contact region ranges from 500 $\mu\Omega$ to 750 $\mu\Omega$ for a new and a degraded contact, respectively. For samples B and C, the resistance of the arcing contact region ranges from 80 $\mu\Omega$ to 160 $\mu\Omega$ for a new and a degraded contact, respectively.

Then, for the fuzzy analysis, the minimum and maximum ranges established for CB-A contact resistance values were $R_m = [150, 300]$ and $R_a = [500, 750]$, while, for CB-B and CB-C, they were $R_m = [40, 80]$ and $R_a = [60, 120]$. Table 1 presents the parameters of ($R_{m1} \dots R_{m5}$, $R_{a1} \dots R_{a5}$) for the linguistic variables input for each sample type.

To quantify the degradation level, five linguistic output variables were established and defined as follows: Low Degradation (DL-L); Moderately Low Degradation (DL-ML); Median Degradation (DL-M); Moderately High Degradation (DL-MH); and High Degradation (DL-H). In Figure 11, a graphic illustration of the membership functions for the output variables is shown.

Table 1. Parameters limits of Rm and Ra for CB-A, CB-B, and CB-C.

Parameters	CB-A	CB-B	CB-C
Rm1	150.0	40	40
Rm2	187.5	50	50
Rm3	225.0	60	60
Rm4	262.5	70	70
Rm5	300.0	80	80
Ra1	500.0	60	60
Ra2	562.5	75	75
Ra3	625.0	90	90
Ra4	687.5	105	105
Ra5	750.0	120	120

In the proposed system, weights W_m and W_a are assigned to Rm and Ra, respectively, to take into consideration the CB operating condition and how significant the degradation of each contact part is. As a rule, if the degradation of Rm is greater than Ra, W_m is used; otherwise, W_a is used. An exception is created when the contact is initially classified as highly degraded (H) since, in this case, a different weight is not imposed. The set of rules has been set according to the fuzzy relationship matrix presented in Table 2.

Table 2. Fuzzy relationship matrix.

	Ra = L	Ra = ML	Ra = M	Ra = MH	Ra = H
Rm = L	DL = L	DL = $W_a \times ML$	DL = $W_a \times M$	DL = $W_a \times MH$	DL = H
Rm = ML	DL = $W_m \times ML$	DL = ML	DL = $W_a \times M$	DL = $W_a \times MH$	DL = H
Rm = M	DL = $W_m \times M$	DL = $W_m \times M$	DL = M	DL = $W_a \times MH$	DL = H
Rm = MH	DL = $W_m \times MH$	DL = $W_m \times MH$	DL = $W_m \times MH$	DL = MH	DL = H
Rm = H	DL = H	DL = H	DL = H	DL = H	DL = H

The inference process adopted in the proposed system was the max–min, with the output defuzzification method being the Mean of Maximum (MoM). For the proposed system, the set of rules was defined as:

1. If Rm = L and Ra = L, then DL = L;
2. If Rm = L and Ra = ML, then DL = ML
3. If Rm = L and Ra = M, then DL = M;
4. If Rm = ML and Ra = L, then DL = ML;
5. If Rm = ML and Ra = ML, then DL = ML;
6. If Rm = ML and Ra = M, then DL = M;
7. If Rm = M and Ra = L, then DL = M;
8. If Rm = M and Ra = ML, then DL = M;
9. If Rm = M and Ra = M, then DL = M;
10. If Rm \neq H and Ra = MH, then DL = MH;
11. If Rm = MH and Ra \neq H, then DL = MH;
12. If Rm = H or Ra = H, then DL = H.

3. Results and Discussion

To classify the contact degradation levels, DRM tests were performed on CB-A, CB-B, and CB-C. To quantify the degradation levels, the parameters Rm and Ra were extracted from the DRM curves following the procedure described in Section 2.1. The curves were obtained at the rated contact opening speed and under application of a test current of 300 A. The tests were performed using the arrangement designed and developed in this research. Figures 12 and 13 show the DRM curves obtained for each CB pole.

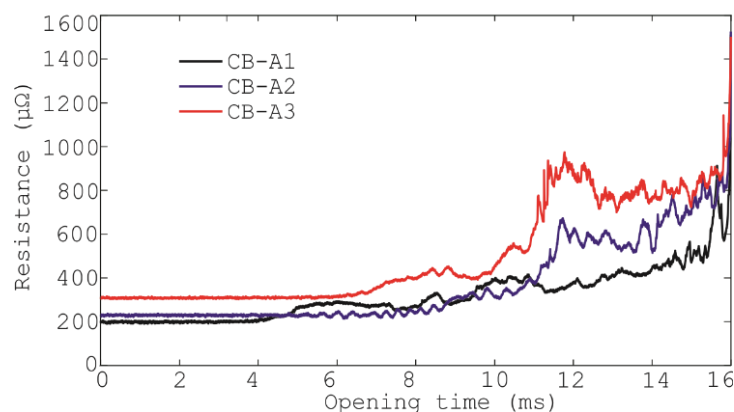


Figure 12. Curves of DRM for the samples CB-A1, CB-A2, and CB-A3, obtained at rated contact opening speed and current of 300 A.

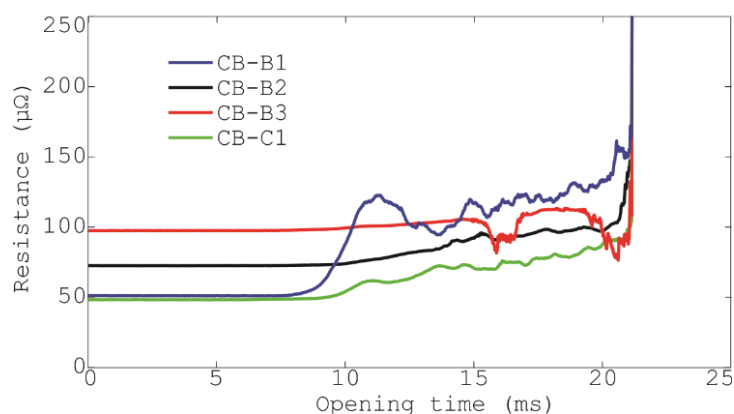


Figure 13. Curves of DRM for the samples CB-B1, CB-B2, CB-B3, and CB-C1, obtained at rated contact opening speed and current of 300 A [34].

Analyzing the DRM curves obtained for CBs A and B, and comparing the three curves to each other, one can observe that there are different degradation levels among the three contacts of each CB even though they belong to the same breaker and are basically subjected to the same load conditions. Additionally, upon reviewing the DRM results of CB-A, it is evident that the contact CB-A3 exhibited a higher degradation level. Both the arcing and main contact regions displayed resistance values surpassing those of the other contacts, as confirmed by visual inspection of the fixed and mobile contacts depicted in Figure 6.

For CB-B, the contact CB-B3 presented significantly higher resistance values in the main contact region. Moreover, it can be observed that all contact samples presented higher resistance values than the new contact used as reference (CB-C1).

From the DRM curves shown in Figure 12, it can be observed that the degradation of the main and arcing contacts (of all contact samples) happened proportionally, that is, the greater the degradation of the main contact, the greater the degradation of the arcing contact. However, the results presented in Figure 13 indicate that this does not necessarily happen in all CBs. The DRM curve for CB-B1, for example, has one of the least degraded main contacts but, at the same time, has the most degraded arcing contacts. The differences between the degradation process of the main and arcing contacts occur due to particular CB usages. In cases of CBs used in industries, for instance, where load current is relatively high and short circuits rarely occur, the main contacts suffer more severe degradation than arcing contacts.

Tables 3 and 4 present a summary of the results obtained in the DRM tests for each contact of CB-A and CB-B, respectively. To quantify the degradation levels, R_m and R_a parameters were extracted from each of the DRM curves according to Figure 3. From the

dataset presented in Tables 3 and 4, a boxplot analysis was carried out. Figures 14–17 present the boxplot for each contact of CB-A and CB-B.

Table 3. Summary of the parameters of the DRM curve for contacts CB-A1, CB-A2, and CB-A3 degraded in service.

DRM Test	Rm ($\mu\Omega$)			Ra ($\mu\Omega$)		
	CB-A1	CB-A2	CB-A3	CB-A1	CB-A2	CB-A3
1	200	228	310	423	543	718
2	198	227	313	430	517	701
3	196	228	314	479	493	686
4	197	228	315	405	531	697
5	198	224	314	477	521	692
6	197	221	315	427	585	676
7	197	220	315	424	541	672
8	193	220	312	418	535	661
9	192	219	314	459	509	631
10	196	219	313	476	529	633

Table 4. Summary of the parameters of the DRM curve for contacts CB-B1, CB-B2, and CB-B3 degraded in service and CB-C1 without significant degradation.

DRM Test	Rm ($\mu\Omega$)				Ra ($\mu\Omega$)			
	CB-B1	CB-B2	CB-B3	CB-C1	CB-B1	CB-B2	CB-B3	CB-C1
1	51	73	104	49	103	91	91	76
2	51	70	102	47	109	95	108	77
3	50	73	101	49	114	94	110	77
4	51	71	102	50	111	93	107	75
5	50	71	94	49	113	90	101	72
6	50	74	103	48	112	96	112	67
7	50	72	91	48	112	90	95	78
8	50	75	97	50	112	94	107	78
9	50	72	97	49	112	90	101	79
10	50	73	85	50	112	88	93	77

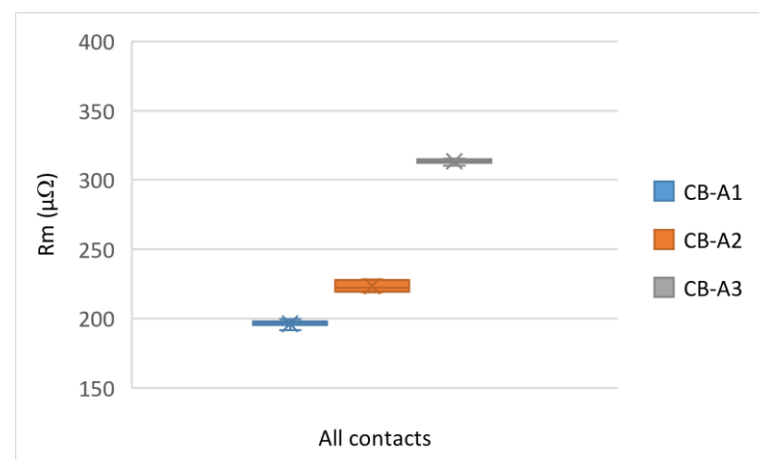


Figure 14. Rm boxplot for samples CB-A1, CB-A2, and CB-A3.

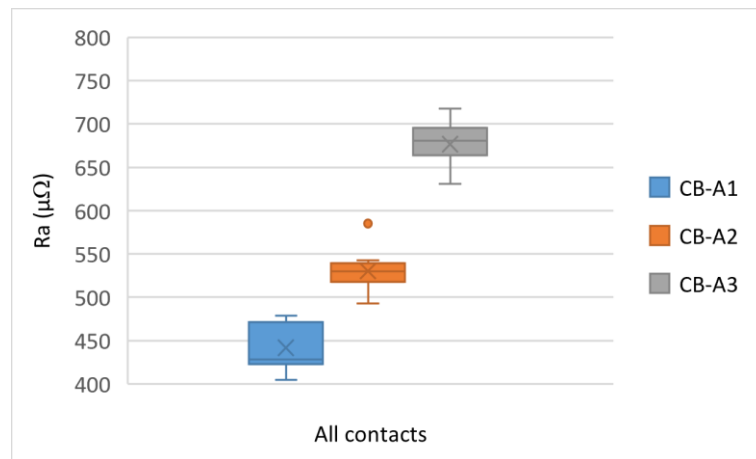


Figure 15. Ra boxplot for samples CB-A1, CB-A2, and CB-A3.

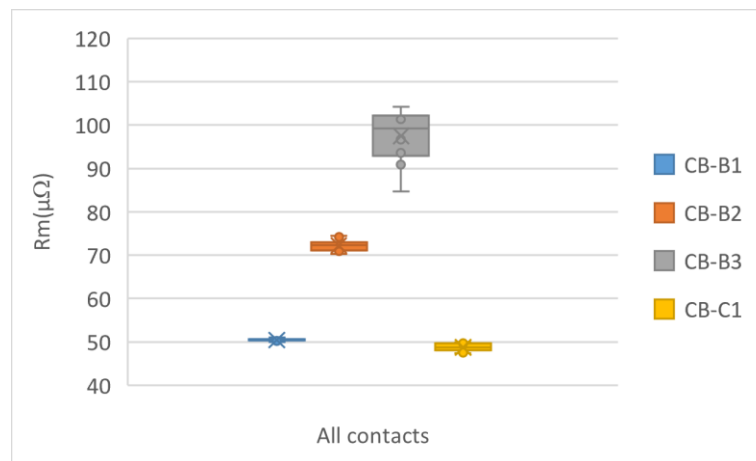


Figure 16. Rm boxplot for samples CB-B1, CB-B2, CB-B3, and CB-C1.

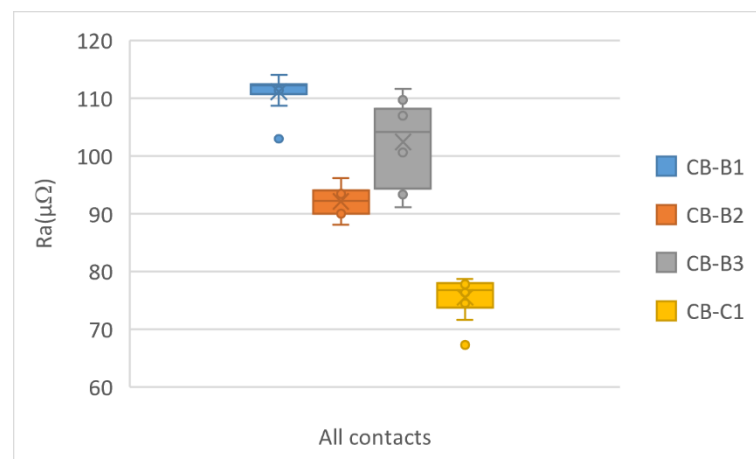


Figure 17. Ra boxplot for samples CB-B1, CB-B2, CB-B3, and CB-C1.

From the results presented in Figures 14–17, it can be observed that the boxplot charts are a good representation of the data behavior. The median or the third quartile can be used as an indicator of contact degradation level. The correlation between the Q3 value and the contact degradation level was confirmed by visual inspections of the contacts.

Additionally, the IQR can also be used as an indicator of the operating state of the CB mechanical system. For highly degraded contacts, the erosion process may change the contact geometry. Therefore, during opening and closing operations, mechanical defects

might cause microseparations of the contacts, generating masked resistance values. Thus, a larger IQR is obtained. Hence, the IQR can be used as an evaluating parameter to detect mechanical defects.

As previously mentioned, the third quartile values of the parameters R_m and R_a , obtained from the boxplot analysis, are the fuzzy system input data. Variations in the median and IQR values can also indicate failures in the CB poles, as will be shown later. Table 5 presents a summary of R_m and R_a for each sample, obtained from the boxplot analysis, along with the degradation level obtained in the fuzzy analysis.

Table 5. Summary of the parameters of the DRM curve and degradation levels for contacts CB-A1, CB-A2, CB-A3, CB-B1, CB-B2, and CB-B3 degraded in service.

Contact	R_m ($\mu\Omega$)	R_a ($\mu\Omega$)	Level of Degradation (%)
CB-A1	198	472	32
CB-A2	228	539	52
CB-A3	314	695	100
CB-B1	50	78	30
CB-B2	73	94	81
CB-B3	102	108	100
CB-C1	50	78	reference

For the proposed fuzzy system, in all cases, $W_m = 1$ and $W_a = 1$ were assigned as each specific part of the contacts has its respective function and, if highly degraded, might cause CB malfunction.

From the results presented in Table 5, it can be observed that the proposed technique successfully provided a quantitative indicator of contact degradation levels, including separated results for the main and arcing contacts.

4. Conclusions

The proposed technique provides a quantitative assessment of CB operational status. The combination of various statistical tools, such as the boxplot and fuzzy logic, enables an evaluation to be conducted without the subjectivity of human decision-making. Therefore, a more objective and reliable diagnosis can be achieved.

Adopting the methodology of obtaining DRM parameters through a sequence of 10 DRM tests enabled the identification of the following DRM result characteristics: each of the 10 curves is similar to each other, as expected, but they are not identical; there is no specific curve that best represents dynamic resistance; and the utilization of the boxplot facilitates the identification of DRM parameters that best represent the operational state of the contact, overcoming the challenge of curve variation between tests. Boxplot charts proved to be valuable visual aids for analyzing dataset behavior. Moreover, the third quartile, also utilized as an input parameter for the fuzzy-logic-based classification system, yielded percentage degradation values consistent with the evaluation obtained by the traditional DRM method.

The proposed technique stands out as being a good asset management tool, providing an objective and non-subjective information regarding CB contact degradation level. However, a prior analysis of the CB model to be analyzed is required since there may be a significant difference in the maximum contact resistance suggested by the equipment manufacturer. Moreover, the classification of contact degradation level provides complementary information to other diagnostic techniques, serving as a tool to support the decision to take equipment out of operation.

Author Contributions: Conceptualization, R.T.S., G.R.S.L. and E.G.C.; methodology, R.T.S., G.R.S.L. and A.C.O.; Formal analysis, R.T.S. and G.R.S.L.; software, R.T.S.; data curation, R.T.S. and A.C.O.; writing—original draft preparation, R.T.S., G.R.S.L., A.C.O. and A.F.L.N.; writing—review and editing, G.R.S.L., E.G.C. and A.F.L.N.; project administration, E.G.C. All authors have read and agreed to the published version of the manuscript.

Funding: The authors are grateful to the Programa de Pós-Graduação em Engenharia Elétrica (PPgEE/UFCEG) and Coordenação de Aperfeiçoamento de Pessoal de Nível Superior—Brasil (CAPES) for the APC payment.

Data Availability Statement: The original contributions presented in the study are included in the article, further inquiries can be directed to the corresponding author.

Conflicts of Interest: The authors declare no conflicts of interest. The funders had no role in the design of the study; in the collection, analyses, or interpretation of data; in the writing of the manuscript; or in the decision to publish the results.

References

1. Ukil, A.; Zlatanski, M.; Hochlehnert, M. Monitoring of HV Generator Circuit Breaker Contact Ablation Based on Acoustic Emission. *IEEE Trans. Instrum. Meas.* **2013**, *62*, 2683–2693. [\[CrossRef\]](#)
2. *IEEE C37.10.1-2000*; Guide for the Selection of Monitoring for Circuit Breakers. IEEE: New York, NY, USA, 2001.
3. Zhong, J.; Li, W.; Billinton, R.; Yu, J. Incorporating a Condition Monitoring Based Aging Failure Model of a Circuit Breaker in Substation Reliability Assessment. *IEEE Trans. Power Syst.* **2015**, *30*, 3407–3415. [\[CrossRef\]](#)
4. Grijp, M.H.; Bedet, J.S.; Hopkins, R.A.; Greyling, J.E. Condition Monitoring of High Voltage Circuit Breaker. In Proceedings of the 4th AFRICON 1996, IEEE AFRICON, Stellenbosch, South Africa, 27 September 1996; pp. 880–885.
5. Huang, L.; Wang, W.; Wu, Z.; Xu, L. Research on the Model of HV SF6 Circuit Breaker Fault Diagnosis Based on Fuzzy Theory. In Proceedings of the Conference Condition Monitoring and Diagnosis, Beijing, China, 21–24 April 2008; pp. 428–431.
6. Razi-Kazemi, A.A.; Niayesh, K. Condition monitoring of high voltage circuit breakers: Past to future. *IEEE Trans. Power Deliv.* **2021**, *2*, 740–750. [\[CrossRef\]](#)
7. Ohlen, M.; Dueck, B.; Wernli, H. Dynamic Resistance Measurements a Tool for Circuit Breaker Diagnostics. In Proceedings of the Stockholm Power Tech International Symposium on Electric Power Engineering, Stockholm, Sweden, 18–22 June 1995; pp. 108–113.
8. Landry, M.; Mercier, A.; Ouellet, G.; Rajotte, C.; Caron, J.; Roy, M.; Brikci, F. A New Measurement Method of the Dynamic Contact Resistance of hv Circuit Breakers. In Proceedings of the Transmission and Distribution Conference and Exhibition, Caracas, Venezuela, 15–18 August 2006; pp. 1–8.
9. Landry, M.; Turcotte, O.; Brikci, F. A complete strategy for conducting dynamic contact resistance measurements on hv circuit breakers. *IEEE Trans. Power Del.* **2008**, *23*, 710–716. [\[CrossRef\]](#)
10. Turcotte, O.; Gauthier, R. A thorough examination of circuit breaker health-hydro-quebec transenergie explores alternative diagnostic methods in its high-voltage circuit breaker maintenance program. *Transm. Distrib. World* **2008**, *60*, 28–33.
11. Jeyaraj, S.G.; Habtay, Y. Effective and Efficient Circuit Breaker Analysis. In Proceedings of the IET Conference on Reliability of Transmission and Distribution Networks, London, UK, 22–24 November 2011; pp. 1–6.
12. Cheng, T.; Gao, W.; Liu, W.; Li, R. Evaluation method of contact erosion for high voltage SF6 circuit breakers using dynamic contact resistance measurement. *Electr. Power Syst. Res.* **2018**, *163*, 725–732. [\[CrossRef\]](#)
13. Stanasic, Z.; Neimanis, R. A New Ultra Lightweight Method for Static and Dynamic Resistance Measurements. In Proceedings of the IEEE International Symposium on Electrical Insulation, San Diego, CA, USA, 6–9 June 2010; pp. 1–4.
14. Sodha, N.S.; Singh, S.; Victor, S.; Tyagi, R.K. Condition Assessment of EHV Class Circuit Breakers Using Dynamic Contact Resistance Measurement Technique. In Proceedings of the CIGRE Session, Paris, France, 26–30 August 2012.
15. Bhole, A.; Gandhare, W. An overview of dynamic contact resistance measurement of hv circuit breakers. *J. Inst. Eng.* **2015**, *4*, 1–8. [\[CrossRef\]](#)
16. Cheng, T.; Zhu, W.; Jin, G.; Yang, Z.; Gao, W. Influence of the injected current on Dynamic Contact Resistance Measurements of HV Circuit Breakers. In Proceedings of the China International Conference on Electricity Distribution (CICED), Shenzhen, China, 23–26 September 2014; pp. 1447–1481.
17. Souza, R.T.; Costa, E.G.; Oliveira, A.C.; Sousa, W.D.V.; Morais, T.C.M. Characterization of Contacts Degradation in Circuit Breakers through the Dynamic Contact Resistance. In Proceedings of the Transmission & Distribution Conference and Exposition-Latin America, Medellin, Colombia, 10–13 September 2014; pp. 1–6.
18. Khoddam, M.; Sadeh, J.; Pourmohamadiyan, P. Performance evaluation of circuit breaker electrical contact based on dynamic resistance signature and using health index. *IEEE Trans. Compon. Packag. Manuf. Technol.* **2016**, *6*, 1505–1512. [\[CrossRef\]](#)
19. Chen, G.; Lan, L.; Pan, Z.; Wen, X.; Wang, Y.; Wu, Y. Electrical erosion test and condition assessment of SF6 CB contact sets. *IET Gen. Trans. Distrib.* **2017**, *11*, 1901–1909. [\[CrossRef\]](#)

20. Liu, Y.; Zhang, G.; Qin, H.; Geng, Y.; Wang, J.; Yang, J.; Zhao, K. Prediction of the dynamic contact resistance of circuit breaker based on the kernel partial least squares. *IET Gen. Trans. Distrib.* **2018**, *12*, 1815–1821. [[CrossRef](#)]
21. Liu, Y.; Zhang, G.; Yang, J.; Zhao, K.; Gao, S. The mathematical model of contact resistance and injected current in DRM tests of SF6 circuit breaker. *IEEE Trans. Compon. Packag. Manuf. Technol.* **2017**, *8*, 82–87. [[CrossRef](#)]
22. Liu, Y.; Zhang, G.; Qin, H.; Liu, W.; Wang, J.; Yang, J. Study on the influence of speed in DRM of SF6 circuit breaker. *Int. J. Electr. Power Energy Syst.* **2020**, *121*, 106067. [[CrossRef](#)]
23. Sun, S.; Cong, P.; Wang, Y. Dynamic Resistance Measurement and Contact Ablation Diagnosis System for SF6 Circuit Breaker. In Proceedings of the 2022 China Automation Congress, Xiamen, China, 25–27 November 2022; pp. 5155–5159.
24. Chen, G.; Li, M.; Wang, Q.; Lu, X.; Zhang, S.; Luo, D. The Contact Erosion Characteristics of SF6 Circuit Breaker Based on Dynamic Resistance Measurement Method. *Energy Rep.* **2022**, *8*, 1081–1089. [[CrossRef](#)]
25. Cao, R.; Lv, H.; Wu, X.; Wang, H.; Zhao, P.; Xin, Z.; Liu, H.; Gao, W. Experimental Study on the Relationship Between Ablation of Circuit Breaker Electrical Life and Dynamic Resistance. In Proceedings of the 9th Frontier Academic Forum of Electrical Engineering; Lecture Notes in Electrical Engineering; Springer: Singapore, 2021.
26. Santos Souza, H.F.; Oliveira, A.C.; Xavier, G.V.R.; Santana, H.N.; Costa, E.G.; Ferreira, T.V. Analysis of alternative parameters of dynamic resistance measurement in high voltage circuit breakers. *High Volt.* **2019**, *4*, 197–202.
27. Abdollah, M.; Razi-Kazemi, A.A. Intelligent Failure Diagnosis for Gas Circuit Breakers Based on Dynamic Resistance Measurements. *IEEE Trans. Instrum. Meas.* **2019**, *68*, 3066–3077. [[CrossRef](#)]
28. Walpole, R.E.; Myers, R.H.; Myers, S.L.; Ye, K. *Probability & Statistics for Engineers & Scientists*, 9th ed.; Pearson Education: Boston, MA, USA, 2012.
29. Razi-Kazemi, A.A.; Vakilian, M.; Niayesh, K.; Lehtonen, M. Priority Assessment of Online Monitoring Investment for Power System Circuit Breakers—Part I: Qualitative–Quantitative Approach. *IEEE Trans. Power Del.* **2013**, *28*, 928–938. [[CrossRef](#)]
30. Simões, M.G.; Shaw, I.S. *Controle e Modelagem Fuzzy*; Editora Blucher: São Paulo, SP, Brazil, 2007.
31. Chang, C.S.; Wang, Z.; Yang, F.; Tan, W.W. Hierarchical Fuzzy Logic System for Implementing Maintenance Schedules of Offshore Power Systems. *IEEE Trans. Smart Grid* **2012**, *3*, 3–11. [[CrossRef](#)]
32. Ge, H.; Asgarpoor, S. Reliability evaluation of equipment and substations with fuzzy Markov processes. *IEEE Trans. Power Syst.* **2010**, *25*, 1319–1328.
33. Nemeth, B.; Laboncz, S.; Kiss, I. Condition Monitoring of Power Transformers Using dga and Fuzzy Logic. In Proceedings of the IEEE Electrical Insulation Conference, Montreal, QC, Canada, 31 May–3 June 2009; pp. 373–376.
34. De Souza, R.T.; Da Costa, E.G.; De Oliveira, A.C. Circuit Breaker Contact Diagnostics Based on Dynamic Resistance and Fuzzy Logic. In Proceedings of the International Symposium on High Voltage Engineering, Pilsen, Czech Republic, 23–28 August 2015.
35. Western Area Power Administration. *Power System Maintenance Manual*; Western Area Power Administration: Denver, CO, USA, 1998.

Disclaimer/Publisher’s Note: The statements, opinions and data contained in all publications are solely those of the individual author(s) and contributor(s) and not of MDPI and/or the editor(s). MDPI and/or the editor(s) disclaim responsibility for any injury to people or property resulting from any ideas, methods, instructions or products referred to in the content.